A Platinum Open Access Journal for Organic Chemistry

Paper

Free to Authors and Readers | DOAJ Seal | *Arkivoc* **2026** (6) 202612563

In search of cocrystals and tricrystals of natural products. A sustainable approach

Mónica Hernández-Vergara and Jesús Valdés-Martínez*

Instituto de Química, Universidad Nacional Autónoma de México, Circuito Exterior, Ciudad Universitaria, 04510, Coyoacán, Ciudad de México, México

Email: jvaldes@iquimica.unam.mx

Received 02-12-2026 **Accepted** 04-04-2026 **Published on line** 04-13-2026

Abstract

A series of ternary multicomponent solids consistent with cocrystals formed by caffeine (CAF), isoniazid (INH), and aliphatic dicarboxylic acids (Cn, n = 3–10) were synthesized using a solvent-free melting method. The dicarboxylic acids acted as bifunctional linkers, capable of hydrogen bonding with both coformers. The resulting solids were characterized using Fourier-transform infrared spectroscopy (FTIR), Differential Scanning Calorimetry (DSC), Thermogravimetric Analysis (TGA), Powder X-ray Diffraction (PXRD), and solid-state ^{13}C Nuclear Magnetic Resonance Spectroscopy (ssNMR). These techniques consistently indicate the formation of new crystalline phases. In particular, shifts in the vibrational and carbonyl signals support the presence of specific hydrogen-bonding motifs. These results confirm the feasibility of obtaining ternary cocrystals using a sustainable, solvent-free method.

Keywords: Cocrystal, dicarboxylic acid, caffeine, isoniazid, melt synthesis.

Introduction

The design, synthesis, and properties of cocrystals, as well as their fundamental definitions, have been extensively studied.[1-8] The growing interest in cocrystals stems from their ability to elucidate the influence of intermolecular interactions on crystalline packing, thereby affecting material properties. Cocrystals also have significant practical and economic value, particularly in the pharmaceutical industry. [9-12]

Although numerous studies have reported new cocrystals, only a few have successfully incorporated three or more components into them. Stabilizing multiple molecular species within a single crystal lattice without covalent bond formation is a significant challenge, often owing to competing interaction preferences and entropic effects. This study specifically addresses this issue by systematically exploring dicarboxylic acid linkers to manage these competing interactions and prevent unintended binary cocrystal formation. Ternary cocrystals are of particular interest in the pharmaceutical industry because of their chemical diversity, which enables the exploration of diverse synthetic strategies for their preparation, including solvent-assisted methods. The design of ternary cocrystals requires careful consideration of the prevention of unintended binary cocrystal formation. While existing strategies have focused on specific binding rules or statistical approaches, this study introduces a novel systematic exploration of homologous dicarboxylic acid linkers. We hypothesized that these bifunctional linkers would mediate interactions in a predictable manner, providing a more controlled pathway to prevent binary co-crystallization and ensure a well-defined ternary phase. Achieving a well-defined ternary phase requires a precise balance of intermolecular interactions to ensure selectivity and stability.[9, 13] Beyond their potential applications, many of which remain unexplored, the development of ternary cocrystals presents an intellectual challenge and an opportunity to advance the crystal engineering methodologies.

The first report on cocrystals containing more than two coformers was published by Aakeröy et al.[1, 9] They applied Etter's hydrogen-bonding rules[14], which state that the strongest hydrogen bond donor pairs with the strongest acceptor, whereas the second strongest donor binds to the second strongest acceptor. Following this principle, they selected isonicotinamide as the core molecule because of its two distinct binding sites, pyridine and amide. In their study, the stronger acid formed a COOH···Npy interaction at one end, whereas the weaker acid participated in an amide-acid heterosynthon.

An alternative strategy for obtaining ternary cocrystals was introduced by Nangia, who employed the statistical cocrystallization of 1,3,5-cyclohexanetricarboxylic acid with a bipyridine mixture.[15] Another approach is supramolecular homologation, which involves the incorporation of an additional molecule into a pre-existing supramolecular homosynthon. Desiraju et al. demonstrated that this strategy can effectively yield ternary cocrystals by simultaneously utilizing hydrogen and halogen bonding.[9, 16] Notably, both Desiraju and Nangia's groups successfully obtained cocrystals with more than three components.

From a crystal-engineering perspective, systematic screening of multicomponent systems using complementary solid-state techniques represents a valuable strategy for identifying new crystalline phases and exploring supramolecular compatibility between molecular components. In this work, we explore the CAF–INH–Cn systems (n = 3–10) using a solvent-free melt approach as a rapid and environmentally friendly method for screening the formation of solid phases consistent with ternary cocrystals. We aimed to demonstrate the feasibility of forming three-component systems predictably by leveraging the well-established cocrystallization tendencies of these components with carboxylic acids[17-25].

Caffeine has frequently been employed as a model compound in pharmaceutical cocrystal studies because of its multiple carbonyl groups, which serve as reliable hydrogen-bond acceptors that form predictable supramolecular synthons with a variety of donors. Likewise, isoniazid contains both hydrogen-bond donor and acceptor functionalities, including an amide group and a pyridine nitrogen, enabling robust intermolecular

interactions. Dicarboxylic acids are particularly attractive coformers in this context because their carboxylic groups can establish strong O–H···N and O–H···O hydrogen bonds. The combination of these complementary functional groups makes the CAF–INH–Cn systems promising candidates for forming ternary multicomponent solids, in which the diacid may act as a supramolecular linker between caffeine and isoniazid molecules.

The use of a homologous series of aliphatic dicarboxylic acids (Cn, n = 3–10) also provides an opportunity to explore how the length of the carbon spacer influences the formation of ternary multicomponent assemblies. In crystal engineering, homologous series are frequently employed to evaluate the transferability and robustness of supramolecular synthons, since gradual changes in molecular geometry can affect hydrogen-bond distances and packing arrangements. In current systems, increasing the length of the diacid chain may modulate the molecule's ability to bridge caffeine and isoniazid via hydrogen bonding, thereby influencing the formation and stability of the resulting multicomponent solids.

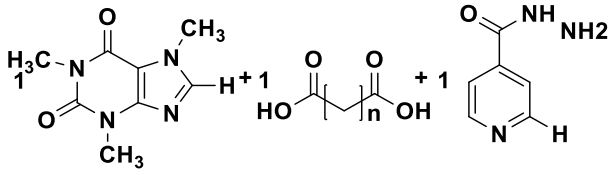

Scheme 1. Reaction scheme for the synthesis of ternary cocrystals comprising caffeine, dicarboxylic acid, and isoniazid in a 1:1:1 stoichiometry (n =1 to n = 8).

The formation of ternary solids in the CAF–INH–Cn systems can be understood in terms of supramolecular synthon complementarity. Caffeine contains multiple carbonyl groups that act as hydrogen-bond acceptors, whereas isoniazid provides both donor (–NH) and acceptor sites (pyridine N and amide C=O). Aliphatic dicarboxylic acids are strong hydrogen-bond donors that commonly form robust O–H···N and O–H···O heterosynthons with pyridine and carbonyl groups. The combination of these components, therefore, allows the possibility of cooperative hydrogen-bond networks in which the diacid may act as a linker between CAF and INH molecules. From a crystal-engineering standpoint, this complementarity provides a plausible supramolecular basis for the formation of the ternary solid phases observed experimentally. Such complementarity has been widely exploited in the design of multicomponent crystals[26,27].

Results and Discussion

The melting points of caffeine, isoniazid, and the selected dicarboxylic acids were sufficiently low to permit melting without decomposition, making the melt method suitable for the synthesis. Stoichiometric amounts of caffeine (CAF), isoniazid (INH), and the corresponding dicarboxylic acid (Cn, where n denotes the number of carbon atoms in the acid) were placed in a vial and heated with a heat gun until complete melting occurred (Scheme 1). Dicarboxylic acids with n = 3–10 were investigated, and the resulting solids were characterized using powder X-ray diffraction (PXRD), Fourier-transform infrared (FTIR) spectroscopy, solid-state nuclear magnetic resonance (ssNMR) spectroscopy, thermogravimetric analysis (TGA), and differential scanning calorimetry (DSC). Subsequent analyses were conducted on systems that incorporated pimelic acid (n = 7). To enable direct comparisons, the binary cocrystals CAF–pimelic acid, INH–pimelic acid, and INH-CAF were independently synthesized and characterized, in addition to a physical mixture of the reagents CAF-pimelic acid-INH.

Attempts were made to obtain single crystals suitable for X-ray diffraction from molten mixtures through controlled cooling and partial melting experiments. In all cases, the products solidified as microcrystalline or polycrystalline materials, preventing isolation of crystals of sufficient size and quality for diffraction analysis. This behavior is consistent with rapid nucleation processes commonly observed during melt crystallization. Consequently, the structural features of the materials were investigated using complementary solid-state techniques including PXRD, FT-IR spectroscopy, DSC/TGA, and solid-state ^{13}C CP/MAS NMR.

Melting Point

Table 1 compares the melting points of the synthesized solids with those of the starting materials. The observed differences in melting points, which diverged from those of the cocrystal materials and mixtures, indicate the formation of new solid phases with distinct crystalline packings and intermolecular interactions between the components. Some compounds, such as CAF-C5-INH, exhibited melting points within the range of their component melting points, whereas others had lower melting points. The decrease in melting temperature alone cannot be considered definitive evidence for cocrystal formation, since eutectic behavior may produce similar effects. However, when considered together with the changes observed in PXRD patterns, FT-IR spectra, and solid-state ^{13}C CP/MAS NMR, the thermal behavior supports the formation of new multicomponent solid phases. The DSC measurements were consistent with those obtained using the Fisher-Johns apparatus.

Table 1. Synthesis of ternary caffeine (CAF)–dicarboxylic acid (Cn)–isoniazid (INH) crystals. Melting points of reactants and products. Mp (CAF): 234 – 236 °C. Mp (INH): 171 – 173 °C

Compound	Melting point of carboxylic acids (°C)	Compound melting point (°C)
CAF–C3–INH	135 – 137	164 – 173
CAF–C4–INH	185 – 188	150 – 160
CAF–C5–INH	95 – 98	110 – 120
CAF–C6–INH	151 – 154	125 – 145
CAF–C7–INH	103 – 105	85 – 100
CAF–C8–INH	140 – 144	120 – 130
CAF–C9–INH	109 – 111	140 – 150
CAF–C10–INH	133 – 137	135 – 150

The binary cocrystals exhibited the following melting points: 90-120 °C for CAF-C7, 105-135 °C for INH-C7, and 150-160 °C for CAF-INH. These values did not match the melting point of CAF-C7-INH. In the physical mixture of the reagents, two distinct melting points were observed: 92-100 °C, corresponding to the acid's melting point, and 161-169 °C, corresponding to isoniazid. The melting point of caffeine was not detected because it dissolved in the other two reagents.

Infrared Spectroscopy

To understand cocrystal formation, changes in the vibrational modes of the functional groups were analyzed using FTIR spectroscopy, as these shifts are diagnostic of new hydrogen-bonding interactions. Figure 1 compares the spectra of INH, CAF, the dicarboxylic acid, and the synthesized compounds, such as CAF-C7-INH, while Table 2 lists the selected bands for all the compounds. The spectra differed from those of the individual conformers and exhibited signals from all the components, confirming the formation of new solid phases.

Key hydrogen-bonding interactions were suggested by the observed shifts. In INH, the shifts in the N–H stretching signals suggest that the carbohydrazide group and nitrogen atom of the pyridine ring actively participate in hydrogen bonding. For the dicarboxylic acids, shifts in the carbonyl and hydroxyl (-OH) signals suggested their involvement in hydrogen bonding interactions. Caffeine contributes via its imidazole group, as shifts in the =C–H stretching region indicate. Notably, the carbonyl group of CAF remained largely unaffected, suggesting that it does not actively participate in the formation of strong hydrogen bonds within identified motifs.

Table 2. Comparison of the vibrational frequencies of the functional groups potentially involved in the formation of supramolecular synthons in the individual components and the synthesized compounds

Compound	INH *v*N – H 3300 cm^{-1}	CAF *v*=C–H 3110 cm^{-1}	*v*O–H···O		*v*O–H···N	CAF *v*C=O 1646 cm^{-1}
	Compound obtained	Compound obtained	Dicarboxilic acid	Compound Obtained	Compound obtained	Compound Obtained
	cm^{-1}					
CAF–C3–INH	3424	3179	2569	2569	1955	1647
CAF–C4–INH	3402	3222	2525	2500	1968	1646
CAF–C5–INH	3304	3211	2627	2546	1914	1648
CAF–C6–INH	3304	3198	2640	2539	1926	1648
CAF–C7–INH	3381	3210	2628	2526	1941	1644
CAF–C8–INH	3354	3194	2616	2500	1940	1646
CAF–C9–INH	3415	3203	2640	2500	1968	1644
CAF–C10–INH	3324	3218	2569	2487	1924	1646

The FTIR spectrum of CAF-C7-INH (Figure 1), reveals new hydrogen bond signals, including a broad band around ~1900 cm^{-1} attributed to O–H···N interactions. This overtone signal strongly suggests that the pyridine ring of INH engages in hydrogen bonding rather than acid molecules bonding exclusively with one another. Additionally, broad signals indicative of O–H···O hydrogen bonds were observed, which were shifted relative to the free acid signal, confirming the involvement of the acid.

These findings are consistent with the hypothesis of cocrystal formation, as evidenced by the spectral shifts and the appearance of new signals. Although spectroscopic evidence strongly indicates cocrystal formation, the absence of single-crystal X-ray diffraction data precludes a definitive determination of the exact three-dimensional arrangement and specific hydrogen-bonding network within the lattice. While our data are consistent with the proposed motifs, full structural elucidation remains a critical next step to conclusively confirm the supramolecular architecture.

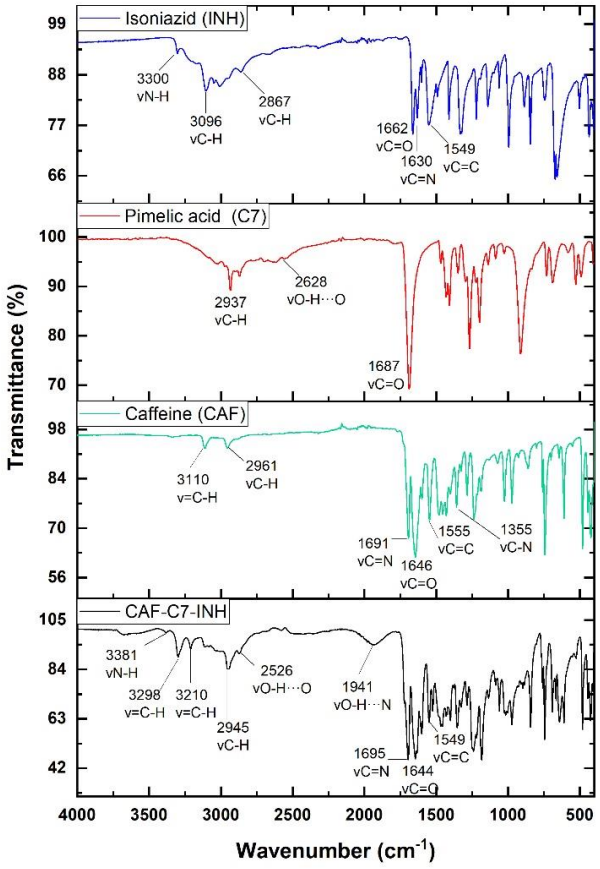

Figure 1. FT-IR spectra of isoniazid, caffeine, pimelic acid, and CAF-C7-INH.

Figure 2 presents a comparison of the spectra of the binary cocrystals CAF-C7, INH-C7, and CAF-INH, the physical mixture of the reagents CAF-C7-INH M, and cocrystal CAF-C7-INH. The spectra of CAF-C7-INH M, CAF-C7, and CAF-INH were different from that of CAF-C7-INH. While the spectrum of INH-C7 resembles that of the CAF-C7-INH compound, a closer inspection of the 2000–400 cm-1 range reveals that the spectra are not identical to each other. Therefore, the resulting product was a ternary rather than a binary co-crystal.

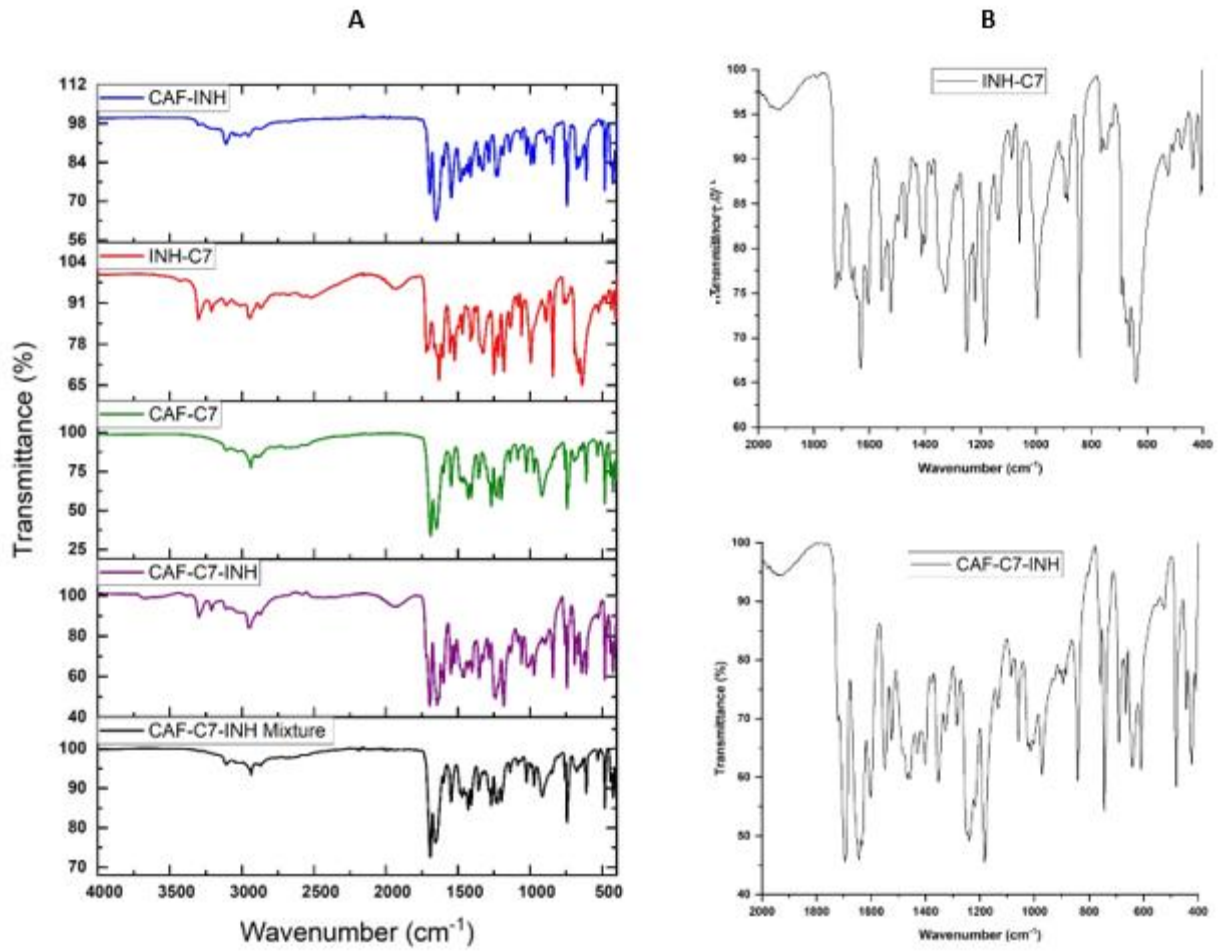

Figure 2. A: A comparison of the infrared spectra of the binary cocrystals CAF-INH, INH-C7, and CAF-C7, the synthesized compound, and the reactant mixture. B: A magnified view of the spectra for INH-C7 and CAF-C7-INH, ranging from 2000 to 400 cm^{-1}.

A schematic representation of possible intermolecular interactions in the ternary systems is shown in Figure 3. In these assemblies, the dicarboxylic acid may act as a hydrogen-bond donor toward the pyridine nitrogen of isoniazid through O–H···N interactions, while the amide N–H group of isoniazid may interact with the carbonyl groups of caffeine via N–H···O hydrogen bonds. Such cooperative interactions could generate supramolecular networks linking the three molecular components. Although the precise arrangement cannot be established without single-crystal diffraction data, the spectroscopic shifts observed in FT-IR and solid-state NMR are consistent with the presence of these hydrogen-bonding motifs.

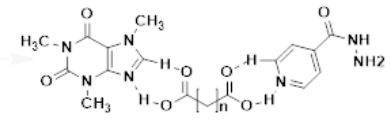

Figure 3. Proposed supramolecular assembly in the CAF–INH–Cn systems illustrating possible hydrogen-bond interactions between caffeine (CAF), isoniazid (INH), and the dicarboxylic acid (Cn). The carboxylic acid group may form O–H···N hydrogen bonds with the pyridine nitrogen of INH, while N–H···O interactions between INH and the carbonyl groups of caffeine can contribute to the formation of an extended hydrogen-bond network.

This schematic representation illustrates plausible intermolecular interactions consistent with the spectroscopic observations.

Such heterosynthons between carboxylic acids, pyridine groups, and amide functionalities are commonly observed in multicomponent crystals. The simultaneous participation of caffeine, isoniazid, and dicarboxylic acid in the hydrogen-bonding network, as suggested by the spectroscopic data, is consistent with the formation of ternary supramolecular assemblies. In the context of crystal engineering, such assemblies are commonly described as tricocrystals or ternary cocrystals when three neutral molecular components are incorporated within a single crystalline phase.

Gas Chromatography – Mass Spectrometry

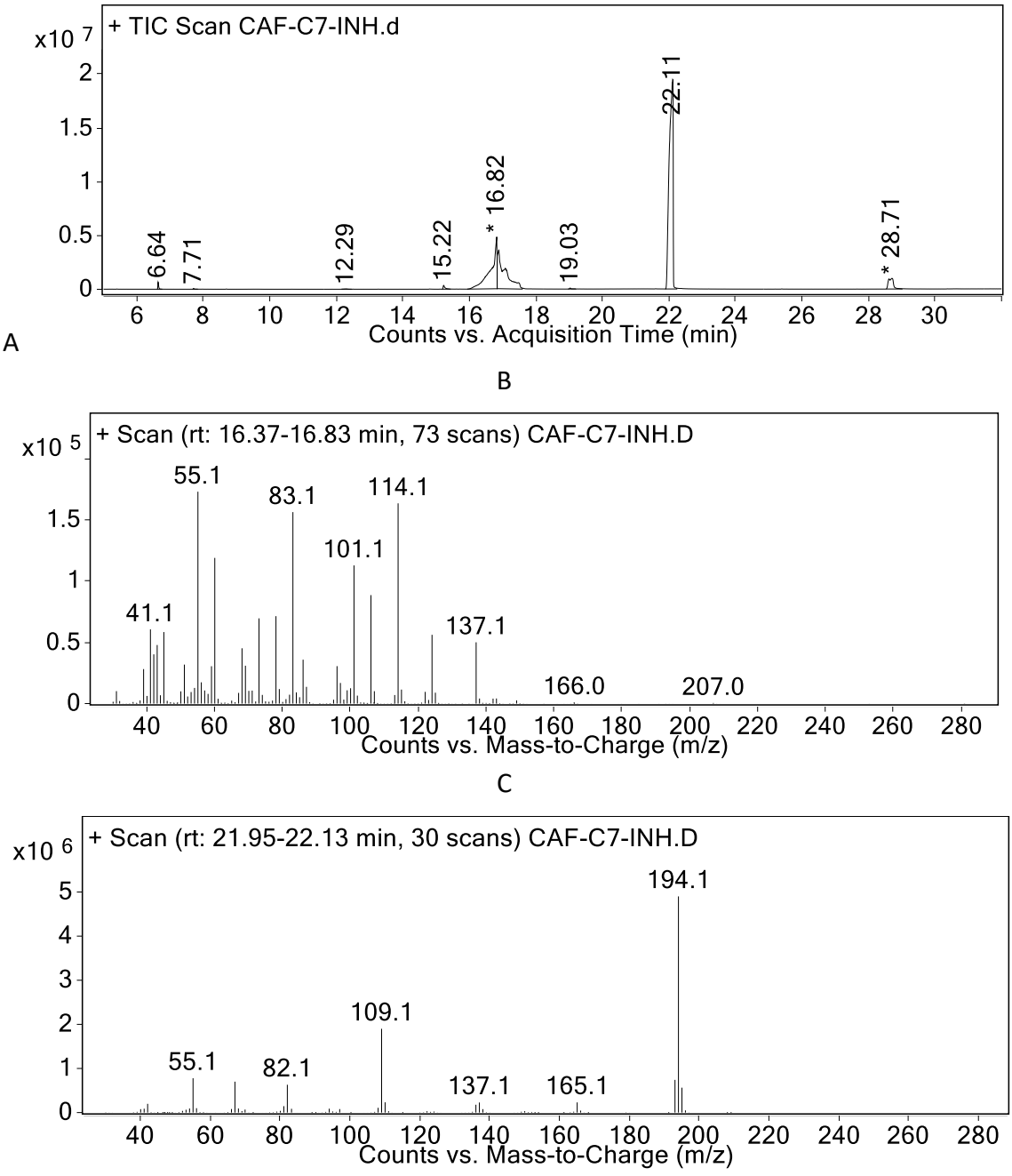

Figure 3. Gas chromatography-mass spectrometry analysis of CAF-C7-INH.

GC/MS analysis was performed to identify the molecules present in the isolated compounds. Figure 3A shows the chromatogram of CAF-C7-INH, which was obtained from Figures 3B and 3C, illustrating the acquisition times at which the molecules of interest were detected: pimelic acid (16.82 min, 160.17 g/mol), isoniazid (16.89 min, 137.14 g/mol), and caffeine (22.11 min, 194.19 g/mol). The compound identification list (Figure 4) confirmed the presence of these compounds in the sample.

Tiempo	Nombre	Match	Área	Fórmula	% Área
6.64	Hexylene glycol	96.9	1142036.78	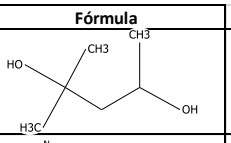	0.40
7.71	3-Pyridinecarbonitrile	96.6	171095.46	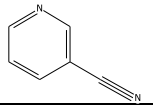	0.06
12.29	4-Pyridinecarboxylic acid	90	211385.3	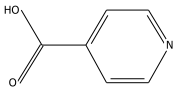	0.07
15.22	4-Pyridinecarboxamide	98.1	1402370.9	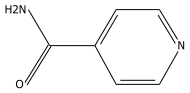	0.49
16.82	Heptanedioic acid	95	57147377.89	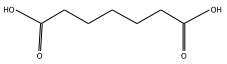	20.07
16.89	Isoniazid	97.4	57137896.41	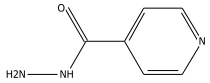	20.07
19.03	No identificado		302933		0.11
22.11	Caffeine	96.3	156563957.3	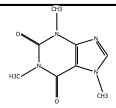	54.98
28.71	Hydrazine, 1,2-diisonicotinoyl-	93.2	10679956.38	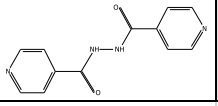	3.75
			284759009.4		100

Figure 4. Compounds identified by GC/MS analysis.

Table 3. The synthesized compounds were analyzed using gas chromatography-mass spectrometry (GC-MS)

Compound	Acquisition time	Identified molecules
CAF–C3–INH	16.48	isoniazid
	21.65	caffeine
	11.72	succinic acid
CAF–C4–INH	16.35	Isoniazid
	21.56	caffeine
	13.39	glutaric acid
CAF–C5–INH	16.62	isoniazid
	21.58	caffeine
	14.9	adipic acid
CAF–C6–INH	16.76	isoniazid
	21.59	caffeine
	16.82	pimelic acid
CAF–C7–INH	16.89	isoniazid
	22.11	caffeine
	17.48	suberic acid
CAF–C8–INH	16.76	isoniazid
	21.58	caffeine
	16.44	isoniazid
CAF–C9–INH	18.7	azelaic acid
	21.56	caffeine
	16.37	isoniazid
CAF–C10–INH	19.94	Sebacic acid
	21.56	caffeine

Thermal Analysis

To obtain additional evidence, we conducted thermal analyses of the formation of the ternary cocrystals. Figure 5 shows the thermal analysis of CAF-C7-INH. The brown and black curves correspond to the DSC and TGA analyses, respectively. In the DSC analysis, an endothermic peak was observed at 93.3 °C, which did not correspond to the melting points of any of the starting reagents (m.p. of caffeine: 234–236 °C, m.p. of pimelic acid: 103–105 °C, and m.p. of isoniazid: 171–173 °C). At this temperature, no mass loss was observed in the TGA curve, indicating that this endotherm was associated with a physical change. Consequently, this peak was attributed to the melting point of CAF-C7-INH.

A second endothermic peak was observed at 146.9 °C, distinct from the melting points of the reagents. Given the absence of mass loss in the TGA curve, this endotherm was tentatively attributed to a solid-solid phase transition, suggesting the potential presence of another polymorphic phase, although definitive confirmation would require further structural analysis. Finally, a change in both the DSC and TGA curves was observed at approximately 270 °C, indicating the thermal decomposition of the solids. The absence of mass loss before the melting temperature in the TGA analysis confirmed that the compound was free of water and solvent inclusions. The melting points obtained from the thermal analyses were consistent with those observed using the Fisher-Johns apparatus.

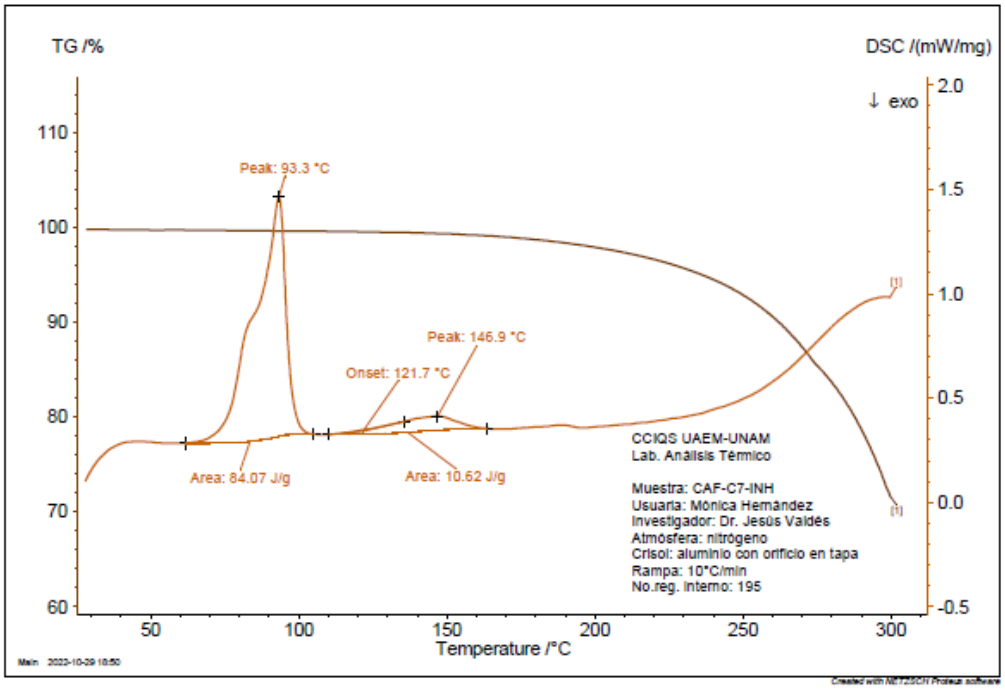

Figure 5. Thermal analysis of CAF-C7-INH. The DSC and TGA curves are shown in brown and black, respectively.

Similar thermal analyses were performed on the binary cocrystal mixtures CAF-C7, INH-C7, CAF-INH, and CAF-C7-INH M mixtures (Figure 6 and 7). The melting points of these compounds were comparable to those of CAF-C7-INH (93.0, 98.8, and 91.2 °C, respectively). However, the thermal behaviors of these compounds differ significantly. For INH-C7 and CAF-C7-INH M, endotherms associated with polymorphic transitions were observed. Notably, INH-C7 exhibited a decomposition temperature above 300 °C, which was higher than those of the other compounds.

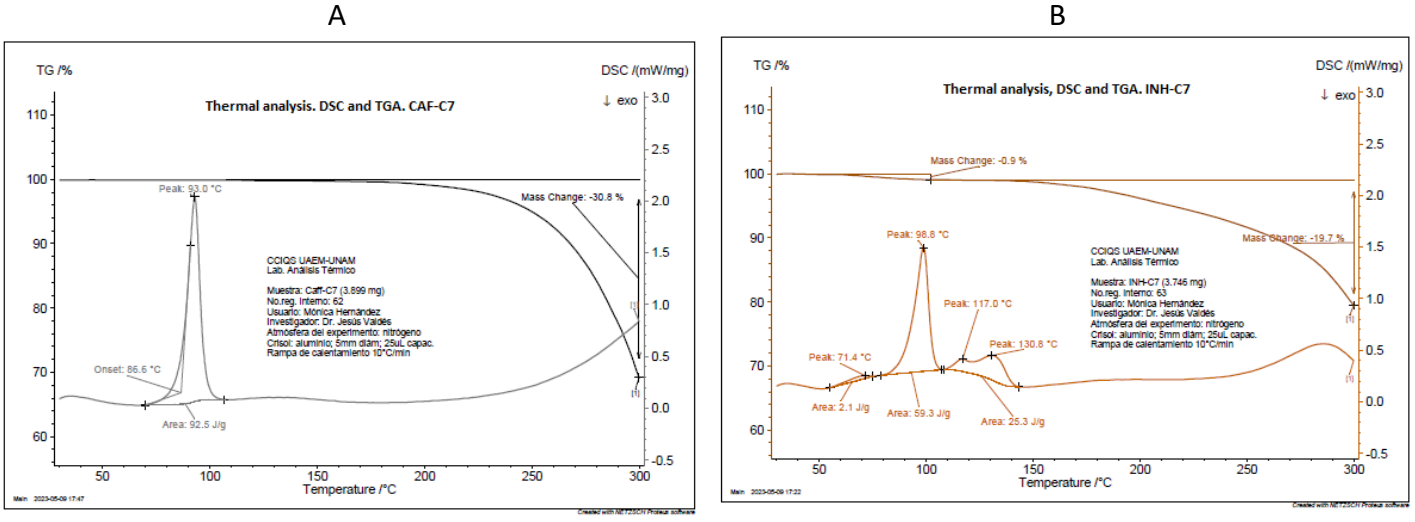

Figure 6. Thermal analyses of the composites were performed using DSC and TGA. A: CAF-C7, B: INH-C7.

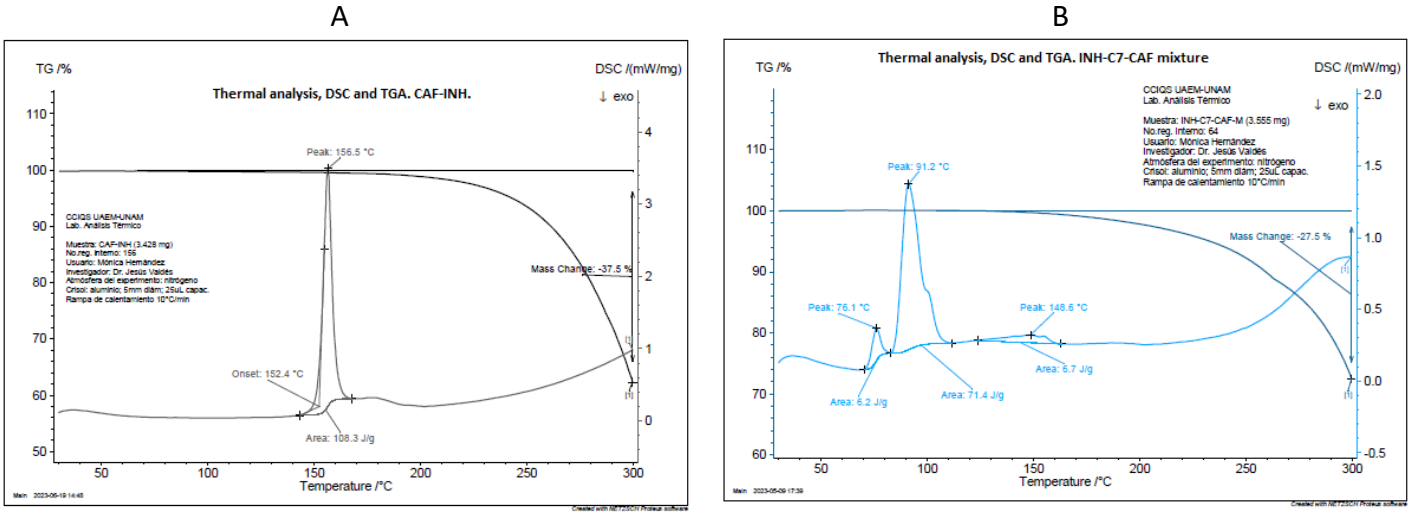

Figure 7. Thermal analyses of the composites were performed using DSC and TGA. A: CAF-INH, B: CAF-C7-INH M.

Table 4 presents the DSC results for all synthesized compounds. The observed melting points, which were generally lower than those of the starting reagents, indicated the formation of new species and supported the hypothesis of cocrystal formation in the solid state.

The observation of multiple endothermic peaks in some samples suggests the potential for polymorphism or the presence of minor, coexisting phases. While our current bulk characterization methods confirm the formation of new phases, the presence of multiple forms could influence the consistency of the physicochemical properties and complicate the definitive assignment of specific structural features from bulk techniques. Fully characterizing these forms, ideally through variable-temperature PXRD or single-crystal analysis, is a critical next step toward a comprehensive understanding of the material properties and represents a current limitation in terms of scope.

Table 4. Melting points and DSC studies of all compounds

Compound	Mp (°C) Carboxylic acids	Mp (°C) Fisher Johns	DSC (°C)
CAF–C3–INH	135 – 137	164 – 173	76.4, 132.3, 157.7
CAF–C4–INH	185 – 188	150 – 160	106.8, 164.1
CAF–C5–INH	95 – 98	110 – 120	106.8, 164.1
CAF–C6–INH	151 – 154	125 – 145	60.7, 107.3, 126.5
CAF–C7–INH	103 – 105	85 – 100	93.3, 146.9
CAF–C8–INH	140 – 144	120 – 130	96.2, 107.3
CAF–C9–INH	109 – 111	90 – 120	73, 84.5
CAF–C10–INH	133 – 137	110 – 135	93.9, 111.7

Powder X-ray diffraction (PXRD)

The PXRD patterns of all the synthesized compounds confirmed the presence of new solid phases. Comparative patterns for isoniazid, dicarboxylic acids (Cn), caffeine, and CAF–Cn–INH (for acids with n = 3–10) are provided in the Supplementary Materials. Figure 8 compares the diffraction patterns of the reagents with those of the CAF–C7–INH cocrystal. The CAF–C7–INH pattern was distinct, exhibiting a single peak at approximately 11° 2θ

(in contrast to the double peak observed for caffeine) and a new intense peak at 25.4° 2θ. These unique diffraction features strongly indicate the formation of a novel crystalline phase with a distinct unit-cell structure. In addition, a comparison of the diffraction patterns of the binary cocrystals (CAF–C7, INH–C7, and CAF–INH), their physical mixture (CAF + C7 + INH), and the CAF–C7–INH composite clearly demonstrated that the ternary compound represented a distinct phase from the binary cocrystals. The relatively broad PXRD reflections are consistent with the materials' microcrystalline nature obtained via melt crystallization.

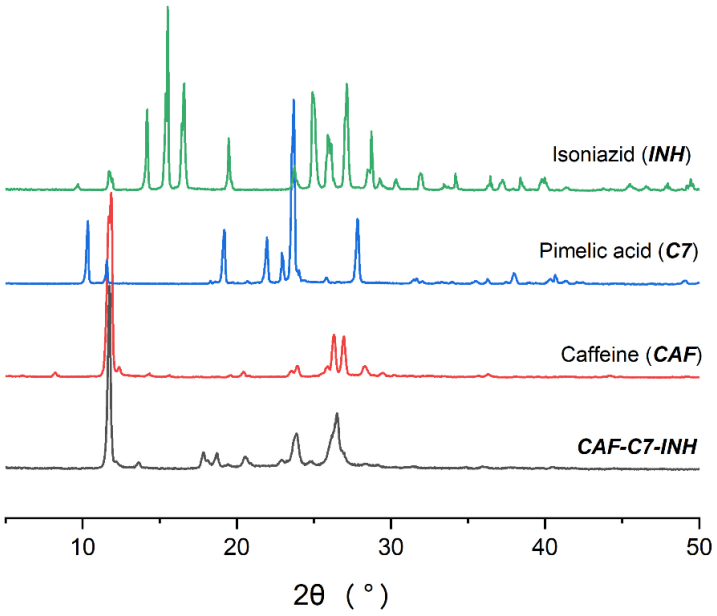

Figure 8. Comparison of powder X-ray diffraction patterns of the reagents and the synthesized compound in the CAF-C7-INH system.

We obtained comparative patterns for the three possible binary cocrystals, CAF-C7, INH-C7, and CAF-INH, a mixture of CAF +C7 + INH and the synthesized CAF-C7-INH composite. The differences in these patterns confirmed the presence of distinct solid phases (Figure 9). Although the IR spectra of INH-C7 are like those of CAF-C7-INH, their diffraction patterns differ significantly, ruling out the possibility that they are the same compound. Although the thermal analyses of CAF-C7 and CAF-C7-INH were similar, their diffraction patterns differed. Thus, CAF-C7-INH was identified as a novel, solid-phase-compound. The diffraction patterns of the products cannot be reproduced by a simple superposition of the individual components' diffraction patterns, indicating that the materials are not physical mixtures but rather new crystalline phases.

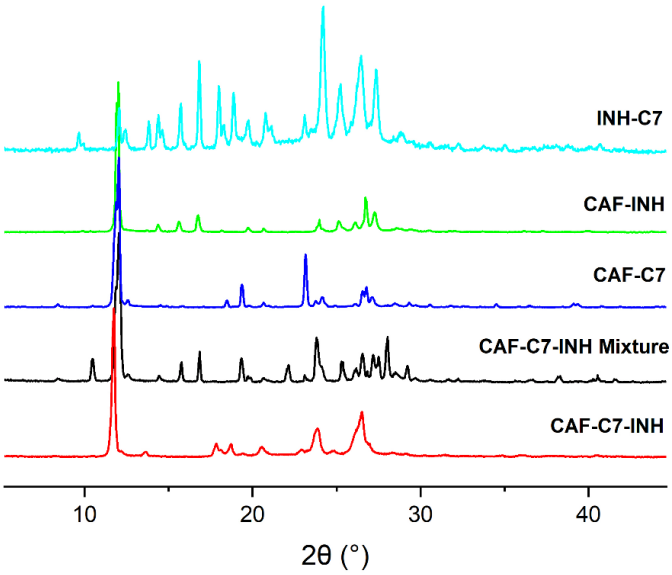

Figure 9. Patterns of the three possible dimeric compounds, CAF-C7, INH-C7, and CAF-INH, a mixture of the three components (CAF + C7 + INH), and the synthesized CAF-C7-INH cocrystal.

The combined characterization results indicate that the products obtained are not simple physical mixtures of the starting materials. The PXRD patterns of the obtained solids differ from those of the individual components and from the corresponding binary systems, while the FT-IR and solid-state ^{13}C CP/MAS NMR spectra show systematic shifts in bands and resonances associated with hydrogen-bonding functionalities. In addition, the thermal analyses reveal melting or transformation events distinct from those of the starting materials. Taken together, these observations are consistent with the formation of new multicomponent solid phases involving caffeine, isoniazid, and the corresponding dicarboxylic acids**.** In solid-state chemistry, the appearance of a PXRD pattern distinct from those of the starting materials and known binary systems, together with consistent spectroscopic and thermal changes, is widely accepted as strong evidence for the formation of a new crystalline phase.

Solid-state nuclear magnetic resonance

Figure 10 shows the ^{13}C CP/MAS NMR spectrum of the CAF–C7–INH compound, along with those of pimelic acid (C7) and caffeine (CAF). All carbon signals expected for the three coformers (INH, CAF, and C7) were observed and assigned based on their magnetic equivalence. Carbonyl signals were observed in the region between 149.6 and 177.8 ppm: caffeine's carbonyls appeared at 154.6 ppm and 149.6 ppm, whereas isoniazid's carbonyl resonated at 168.9 ppm. In contrast, the free acid displayed a single carbonyl signal at 181.2 ppm. In the CAF–C7–INH spectrum, this signal was split into two distinct peaks at 177.8 and 173.0 ppm, which, unlike FT-IR, provides direct, high-resolution evidence of distinct hydrogen-bonding environments for each carbonyl group within the solid lattice. These shifts confirm the formation of hydrogen bonds, and the observed chemical shift ranges are consistent with neutral hydrogen-bonded cocrystals rather than proton-transferred salts, thereby supporting the key features of the proposed supramolecular arrangement, particularly regarding the hydrogen-bonding environments.

The solid-state ^{13}C CP/MAS NMR spectrum of isoniazid was recorded but is not shown in Figure 10 because it exhibits very weak, poorly resolved signals with a low signal-to-noise ratio under the experimental conditions used. Consequently, the spectrum does not provide reliable structural information for comparison. The

discussion is therefore focused on caffeine and the dicarboxylic acids, whose carbonyl resonances allow more meaningful evaluation of changes associated with the formation of the multicomponent solids.

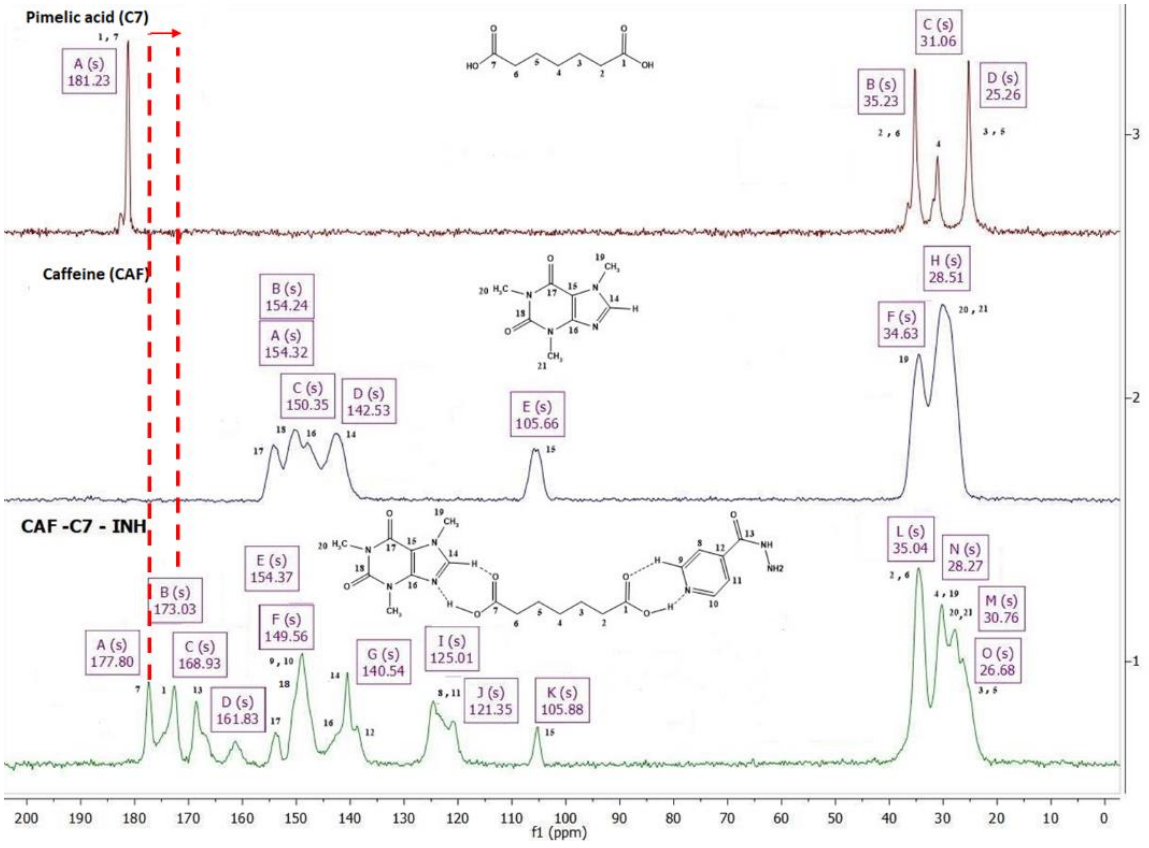

Figure 10. ^{13}C CP/MAS NMR spectrum of ^{13}C (125 MHz) for pimelic acid (C7) and CAF-C7-INH.

The ^{13}C NMR spectrum of CAF-C7-INH was simulated using Spartan software with density functional theory (DFT) at the WB97X-D level and a 6-31G* basis set (Figure 11). The simulated chemical shifts closely matched the experimental data, thereby confirming the accuracy of the results. In the simulation, the carbonyl carbon atoms in the acid were magnetically equivalent, resulting in a single signal at 176.0 ppm.

This simulation confirmed the carbon assignments in the experimental spectrum and validated the presence of the three constituent molecules (CAF, C7, and INH) in the CAF-C7-INH compound.

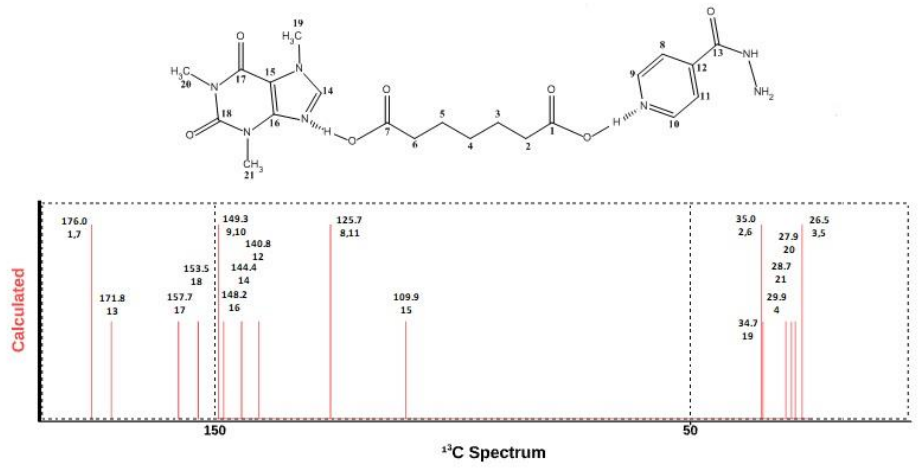

Figure 11. Simulated ^{13}C NMR spectra using Spartan software for the compound CAF-C7-INH.

The ^{13}C NMR spectrum of CAF-C7-INH was simulated using MestreNova (Figure 12). In contrast to the Spartan simulation, MestreNova revealed that the carbonyl carbon signals of the acid were not magnetically equivalent, with two distinct signals observed, which was consistent with the experimental data.

The remaining chemical shifts were consistent with the experimental results, further confirming the proposed assignments and supporting the presence of three molecules (CAF, C7, and INH) in the compound.

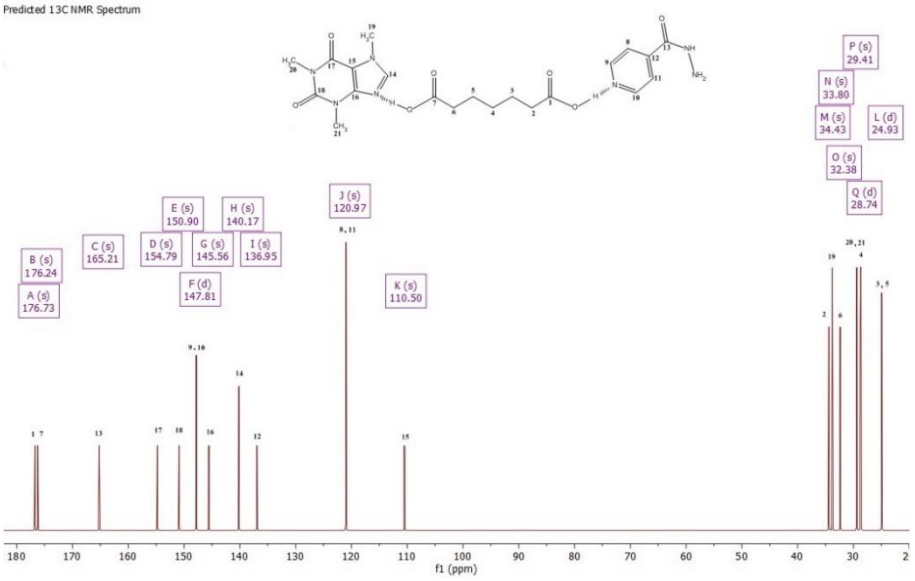

Figure 12. Simulation of the ^{13}C NMR spectrum of CAF-C7-INH using the MestreNova software.

The ^{13}C NMR spectra of the possible binary cocrystals, CAF-C7, INH-C7, and CAF-INH, were analyzed and compared with that of the synthesized compound CAF-C7-INH (Figure 13). The spectral differences confirm the formation of distinct solid phases, thereby identifying CAF-C7-INH as a distinct compound and ruling out the formation of a binary cocrystal.

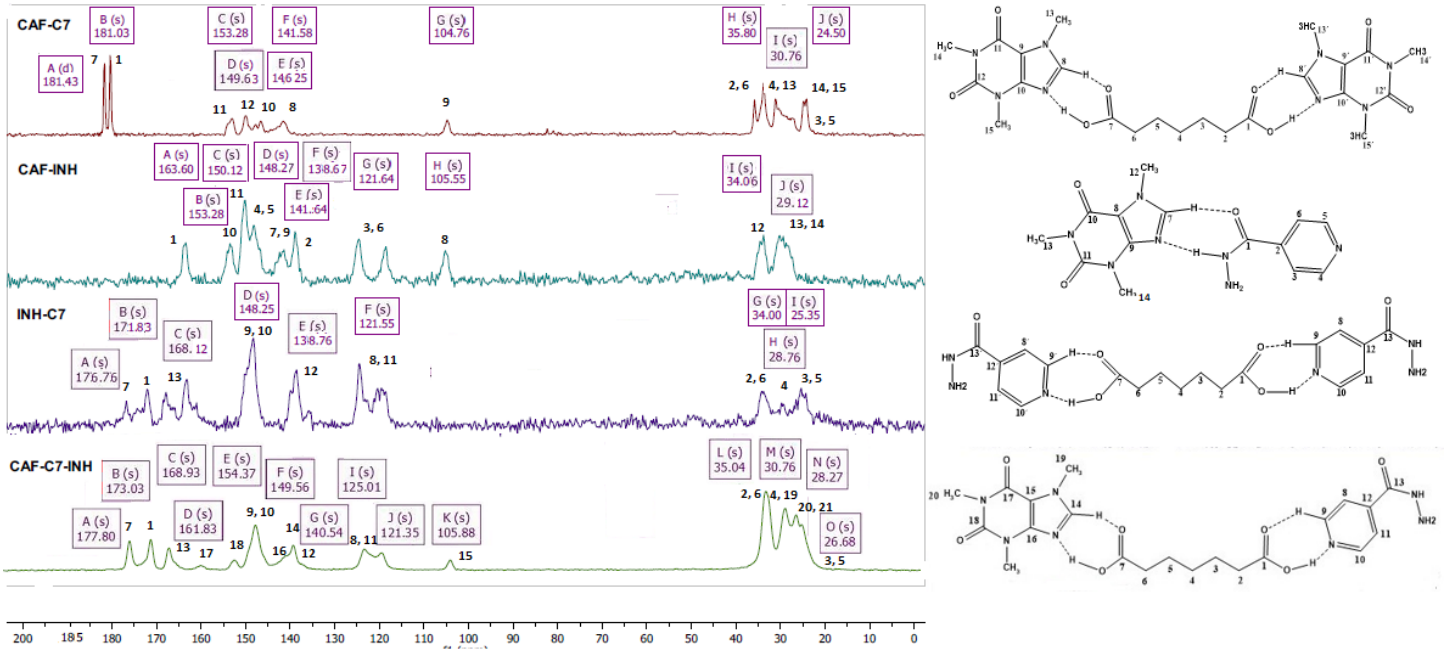

Figure 13. ^{13}C CP/MAS NMR spectra of ^{13}C (125 MHz) for the three possible dimeric compounds, CAF-C7, INH-C7, and CAF-INH, and the compound CAF-C7-INH.

All the synthesized compounds were subjected to ^{13}C CP/MAS NMR spectroscopy. The anticipated signals for the three coformers, INH, CAF, and their corresponding acids, were detected, and the spectra and their assignments are provided in the Supplementary Information. Table 5 presents only the signals attributable to carbonyl groups in the molecules and compares them with those of the carbonyl group in the free acid.

Table 5. Chemical displacements of the carbonyl groups in all compounds

Compound	Carbonyl group displacement (ppm)				
	Free acid	compound		isoniazid	caffeine
CAF-C3-INH	174.4	163.3		163.3	153.7 150.2
CAF-C4-INH	175.8	175.1		165.5	153.4 150.2
CAF-C5-INH	177.7	174.1	167.8	163.8	153.5 150.4
CAF-C6-INH	181.6	181.5	175.6	165.4	154.2 150.2
CAF-C7-INH	181.2	177.8	173.3	168.9	154.4 149.6
CAF-C8-INH	181.2	181.0	177.4	162.8	153.4 149.9
CAF-C9-INH	180.8	180.9	175.6	166.7	153.5 150.1
CAF-C10-INH	181.1	181.9	178.5	165.5	154.4 153.5

The simultaneous changes observed in PXRD patterns, FT-IR spectra, and solid-state ^{13}C CP/MAS NMR demonstrate that the products are not simple physical mixtures of the starting materials. Instead, the data are consistent with the formation of new multicomponent solid phases involving caffeine, isoniazid, and the corresponding dicarboxylic acids.

Conclusions

The present study, therefore, represents a systematic solid-state screening of ternary systems involving caffeine, isoniazid, and a homologous series of aliphatic dicarboxylic acids. The combined PXRD, FT-IR, DSC/TGA, and solid-state NMR data indicate the formation of new multicomponent solid phases across this homologous series. The FTIR spectra showed a broad band around 1900 cm^{-1}, consistent with O–H···N hydrogen bonding, while the ssNMR spectra revealed carbonyl signal splitting, indicative of non-equivalent environments within the cocrystal lattice. These observations are consistent with the formation of neutral hydrogen-bonded cocrystals rather than salts, supporting the plausibility of the proposed supramolecular arrangements depicted in Scheme 1. Although definitive structural determination will require single-crystal X-ray diffraction studies, the combined thermal, spectroscopic, and diffraction data consistently indicate the formation of new multicomponent solid phases within this homologous series. These results demonstrate that melt processing provides a simple and environmentally friendly method for exploring multicomponent crystal formation in pharmaceutically relevant molecular systems.

Experimental Section

Materials. Commercially available caffeine, isoniazid, malonic acid, succinic acid, glutaric acid, adipic acid, pimelic acid, suberic acid, azelaic acid, and sebacic acid were used as received, without further purification. All solvents were of analytical grade and used without further purification.

Instruments. A Varitemp Heat Gun (model UT-750C) was used to fuse the compounds. The melting points were determined using a Fisher-Johns apparatus (Prendo, model PF-300) equipped with an uncalibrated mercury thermometer. FTIR spectra were recorded using a Bruker Tensor 27 and an Agilent Technologies Cary 600 FT-IR spectrometer, both equipped with an ATR accessory, in the 4000–400 cm^{-1} range. Powder X-ray diffraction (PXRD) experiments were performed using a Bruker D8 Advance diffractometer with Bragg–Brentano geometry, Cu Kα radiation, and Lynxeye detector. Thermal analyses were conducted on a Netzsch STA 449 F3 Jupiter simultaneous TGA–DSC instrument using a heating rate of 10 °C/min under a nitrogen atmosphere (99.999%) and aluminum crucibles. OriginPro version 8 was used to process the FTIR and PXRD data, whereas MestReNova version 12.01 was used to analyze the ssNMR spectra.

General Procedures. The melting points of caffeine (234–236 °C), isoniazid (171–173 °C), and the selected dicarboxylic acids permitted the use of the fusion method for cocrystal synthesis. Stoichiometric amounts of caffeine, isoniazid, and the respective dicarboxylic acid were placed in a glass vial and heated using a hot air gun until a homogeneous melt was obtained. The resulting melt was allowed to cool and dry at room temperature. The solidified material was then ground to a fine powder and characterized by melting point determination, powder X-ray diffraction (PXRD), Fourier transform infrared (FTIR) spectroscopy, solid-state nuclear magnetic resonance (ssNMR) spectroscopy, and differential scanning calorimetry (DSC) analyses.

CAF-C3-INH (1). Caffeine (37.3 mg, 0.20 mmol), malonic acid (20.0 mg, 0.20 mmol), and isoniazid (26.3 mg, 0.20 mmol) were placed in a glass vial and heated using a hot-air gun until the solids melted completely. A yellow solid was obtained upon cooling. Melting point**:** 164–173 °C. IR (ATR, cm^{-1}): 3424 (*ν*N-H), 3179 (*ν*=C-H), 1647 (*ν*C=O). RMN ^{13}C CP/MAS (125 MHz), δ(ppm): 163.3 (3C; C-1, C-3, C-9), 153.7 (1C; C-13), 150.2 (3C; C-5, C-6, C-14), 142.2 (1C; C-12), 139.0 (1C; C-10), 136.1 (1C; C-8), 119.7 (2C; C-4, C-7), 105.2 (1C; C-11), 34.4 (1C; C-2), 30.5 (1C; C-15), 28.5 (2C; C-16, C-17).

CAF-C4-INH (2). Caffeine (32.9 mg, 0.20 mmol), succinic acid (20.0 mg, 0.20 mmol), and isoniazid (23.2 mg, 0.20 mmol) were placed in a glass vial and heated using a hot-air gun until the solids melted completely. A yellow crystalline solid was obtained after cooling the mixture to room temperature. Melting point: 150–160 °C. IR (ATR, cm^{-1}): 3402 (*ν*N-H), 3222 (*ν*=C-H), 2500 (*ν*O-H···), 1968 (*ν*O-H···N), 1646 (*ν*C=O). RMN ^{13}C CP/MAS (125 MHz), δ(ppm): 175.1 (2C; C-1, C-4), 165.5 (1C; C-1), 153.4 (1C; C-14), 150.2 (3C; C-6, C-7, C15), 146.8 (1C; C-10), 142.0 (2C; C-9, C-13), 121.9 (2C; C-5, C-8), 105.0 (1C; C-12), 34.1 (1C; C-16), 29.3 (4C; C-2, C-3, C-17, C-18).

CAF-C5-INH (3). Caffeine (29.4 mg, 0.20 mmol), glutaric acid (20.0 mg, 0.20 mmol), and isoniazid (20.8 mg, 0.20 mmol) were placed in a glass vial and heated using a hot air gun until the solids melted. A yellow crystalline solid was obtained upon cooling. Melting point: 110–120 °C. IR (ATR, cm^{-1}): 3304 (*ν*N-H), 3211 (*ν*=C-H), 2546 (*ν*O-H···0), 1914 (*ν*O-H···N), 1648 (*ν*C=O). RMN ^{13}C CP/MAS (125 MHz), δ(ppm): 174.1 (1C; C-5), 167.2 (1C; C-1), 163.8 (1C; C-11), 153.5 (1C; C-15), 150.4 (1C; C16), 146.9 (2C; C-7, C-8), 140.4 (3C; C-10, C-12, C-14), 123.5 (1C; C-6), 122.1 (1C; C-9), 105.1 (1C; C-13), 34.6 (3C; C-2, C-4, C-17), 30.4 (1C; C-19), 28.0 (1C; C-18), 20.2 (1C; C-3).

CAF-C6-INH (4). Caffeine (26.6 mg, 0.20 mmol), adipic acid (20.0 mg, 0.20 mmol), and isoniazid (18.8 mg, 0.20 mmol) were placed in a glass vial and heated using a hot-air gun until the solids melted. A yellow crystalline solid was obtained upon cooling. Melting point: 125–145 °C. IR (ATR, cm^{-1}): 3304 (*ν*N-H), 3198 (*ν*=C-H), 2539 (*ν*O-H···0), 1926 (*ν*O-H···N), 1648 (*ν*C=O). RMN 13C CP/MAS (125 MHz), δ(ppm): 181.5 (1C; C-6), 175.6 (1C; C-1), 165.4 (1C; C-12), 154.2 (1C; C-16), 150.2 (1C; C-17), 147.5 (2C; C-8, C-9), 142.3 (2C; C-13, C-15), 136.4 (1C; C-11), 121.7 (1C; C-7), 116.3 (1C; C-10), 105.0 (1C; C-14), 34.1 (3C; C-2, C-5, C-18), 29.7 (2C; C-19, C-20), 23.8 (2C; C-3, C-4).

CAF-C7-INH (5). Caffeine (24.2 mg, 0.20 mmol), pimelic acid (20.0 mg, 0.20 mmol), and isoniazid (17.1 mg, 0.20 mmol) were placed in a glass vial and heated using a hot air gun until the solids melted completely. A yellow crystalline solid was obtained upon cooling. Melting point: 85–100 °C. IR (ATR, cm^{-1}): 3381 (*ν*N-H), 3210 (*ν*=C-H), 2526 (*ν*O-H···0), 1941 (*ν*O-H···N), 1644 (*ν*C=O). RMN 13C CP/MAS (125 MHz), δ(ppm): 177.8 (1C; C-7), 173.0 (1C; C-1), 168.9 (1C; C-13), 154.4 (1C; C-17), 149.6 (3C; C-9, C-10, C-18), 140.5 (3C; C-12, C-14, C-16), 125.1 (1C; C-11), 121.3 (1C; C-8), 105.9 (1C; C-15), 35.0 (2C; C-2, C-6), 28.3 (2C; C-4, C-19), 30.8 (2C; C-20, C-21), 26.7 (2C; C-3, C-5).

CAF-C8-INH (6). Caffeine (22.3 mg, 0.20 mmol), suberic acid (20.0 mg, 0.20 mmol), and isoniazid (15.7 mg, 0.20 mmol) were placed in a glass vial and heated using a hot air gun until the solids melted. A yellow crystalline solid was obtained upon cooling. Melting point: 120–130 °C. IR (ATR, cm^{-1}): 3354 (*ν*N-H), 3194 (*ν*=C-H), 2500 (*ν*O-H···0), 1940 (*ν*O-H···N), 1646 (*ν*C=O). 13C CP/MAS (125 MHz), δ(ppm): 181.0 (1C; C-8), 177.0 (1C; C-1), 162.8 (1C; C-14), 153.4 (1C; C-18), 149.9 (3C; C-10, C-11, C-19), 141.1 (2C; C-13, C-15), 122.5 (2C; C-9, C-12), 105.0 (1C; C-16), 34.9 (3C; C-2, C-7, C-20), 30.1 (4C; C-4, C-5 C-21, C-22), 24.8 (2C; C-3, C-6).

CAF-C9-INH (7). Caffeine (20.6 mg, 0.20 mmol), azelaic acid (20.0 mg, 0.20 mmol), and isoniazid (14.6 mg, 0.20 mmol) were placed in a glass vial and heated with a hot air gun until the solids melted completely. A yellow crystalline solid was obtained upon cooling. Melting point: 140–150 °C. IR (ATR, cm^{-1}): 3415 (*ν*N-H), 3230 (*ν*=C-H), 2500 (*ν*O-H···0), 1968 (*ν*O-H···N), 1644 (*ν*C=O). RMN 13C CP/MAS (125 MHz), δ(ppm): 180.9 (1C; C-9), 175.6 (1C; C-1), 166.7 (1C; C-15), 150.1 (4C; C-11, C-12, C-19, C-20), 141.5 (3C; C-14, C-15, C-16), 123.9 (2C; C-10, C-13), 105.3 (1C; C-17), 33.5 (8C; C-2, C-4, C-5, C-6, C-8, C-21, C-22, C-23), 28.3 (2C; C-3, C-7).

CAF-C10-INH (8). Caffeine (19.2 mg, 0.20 mmol), sebacic acid (20.0 mg, 0.20 mmol), and isoniazid (13.5 mg, 0.20 mmol) were placed in a glass vial and heated using a hot-air gun until the solids melted. A yellow solid was obtained upon cooling. Melting point: 135–150 °C. IR (ATR, cm^{-1}): 3324 (*ν*N-H), 3218 (*ν*=C-H), 2487 (*ν*O-H···0), 1924 (*ν*O-H···N), 1646 (*ν*C=O). RMN 13C CP/MAS (125 MHz), δ(ppm): 181.9 (1C; C-10), 178.5 (1C; C-1), 165.5 (1C; C-16), 153.5 (2C; C-20, C-21), 149.0 (2C; C-12, C-13), 141.3 (3C; C-15, C-17, C-19), 123.0 (2C; C-11, C-14), 105.5 (1C; C-18), 32.6 (9C; C-2, C-4, C-5, C-6, C-7, C-9, C-2, C-21, C-22), 25.8 (2C; C-3, C-8).

Supplementary Material

The supplementary material contains the FT-IR spectra, thermal analysis (DSC/TGA), powder X-ray diffraction patterns, and solid-state ^{13}C CP/MAS NMR spectra used to characterize the CAF–Cn–INH ternary systems.

Acknowledgements

The authors gratefully acknowledge Adriana Romo Peréz (FTIR, I.Q. UNAM), Uvaldo Hernández Balderas, and Alejandra Núñez Pineda (CCIQS UAEM-UNAM) for their technical support. M. E. García-Aguilera (solid-state NMR, LURMN), M. León, M. Reyes, and E. Tapia (LANCIC-IQ-UNAM). Technical support from the Centro Conjunto de Investigación en Química Sustentable, UAEMex-UNAM (code: JVM-2016) and financial support from the Dirección General de Asuntos del Personal Académico (DGAPA), Universidad Nacional Autónoma de México (grant IN224625), are gratefully acknowledged. MHV also thanks the Secretaría de Ciencia, Tecnología e Innovación (669017) for the graduate studies scholarship.

References

1. Aakeröy, C.B.; Beatty, A.M.; Helfrich, B.A. *Angew. Chem. Int. Ed*. **2001**, *40*, 3240–3242. https://doi.org/10.1002/1521-3773(20010903)40:17<3240::AID-ANIE3240>3.0.CO;2-X
2. Gadade, D.D.; Pekamwar, S.S. Adv. Pharm. Bull. **2016**, 6, 479–494. https://doi.org/10.15171/apb.2016.062
3. Kodrin, I.; Borovina, M.; Šmital, L.; Valdés-Martínez, J.; Aakeröy, C.B.; Đaković, M. *Dalton Trans.* **2019**, *48*, 16222–16232. https://doi.org/10.1039/C9DT03346G
4. Wang, X.; Zhang, K.; Geng, Y.; Sun, Y.; Chen, F.; Wang, L. *J. Molec. Struct.* **2018**, *1165*, 106-119. https://doi.org/10.1016/j.molstruc.2018.03.105
5. Robertson, C.C.; Wright, J.S.; Carrington, E.J.; Hunter, C.A.; Brammer, L. *Chem. Sci*. **2017**, *8*, 5392. https://doi.org/10.1039/C7SC01801K
6. Shang, N.; Zaworoko, M.J. Polymorphic crystal forms and cocrystals in drug delivery systems; John Wiley & Sons; **2010.** https://doi.org/10.1002/0471266949.bmc156
7. Roy, P.; Ghosh, A. *Cryst. Eng. Comm.* **2020**, *22* ,6958–6974. https://doi.org/10.1039/D0CE01276A
8. Aitipamula, S.; Banerjee, R.; Bansal, A. K.; Biradha, K. *Cryst. Growth Des*. **2012**, *12*, 2147−2152.
9. Aakeröy, C.B.; Sinha, *Co-crystals: Preparation, Characterization, and Applications*; The Royal Society of Chemistry, **2018**. https://doi.org/10.1039/9781788012874
10. Krueger, E. L.; Sinha, A. S.; Desper, J.; Aakeröy, C. B. *Cryst. Eng. Comm.* **2017**, *19*, 4605-4614. https://doi.org/10.1039/C7CE01177F
11. Muddukrishna, B. S.; Swapnil, J. D.; Gautham, G. S.; Krishnamurthy, B. *Int. J. App. Pharm*. **2016**, *8*, 32-37.
12. Cysewski, P.; J. Mol. Model. **2017**, *23*:136. https://doi.org/10.1007/s00894-017-3287-y

13. Aakeröy, C. B.; Desper, J.; Smith, M.M., Chem. Comm. **2007**, 3936–3938. https://doi.org/10.1039/b707518a
14. Etter, M. C.; Macdonald, J. C. *Acta Cryst*. **1990** *B46*, 256 – 262. b) Etter, M. C.; J. Phys. Chem. **1991**, *95*, 4601-4610. https://doi.org/10.1021/j100165a007
15. Bhogala, B. R.; Nangia, A. *New J. Chem.* **2008**, *32*, 800-807. https://doi.org/10.1039/b800293b
16. Aakeröy, C. B.; Gunawardana, C. A. *Chem. Comm.* **2018**, *54*, 14047-14060. https://doi.org/10.1039/C8CC08135B
17. Bucar, D.k.; Henry, R. F.; Lou, X.; Duerst, R. W.; MacGillivray, L.R.; Zhang, G. G. Z. *Cryst. Growth Des.* **2009**, 9(4), 1932-1942. https://doi.org/10.1021/cg801178m
18. Trask, A. V.; Motherwell, W. D. S.; Jones, W. *Cryst. Growth Des.* **2005**, 5(3), 1013-1021. https://doi.org/10.1021/cg0496540
19. Leyssens, T.; Springuel, G.; Montis, R.; Candoni, N.; Veesler, S. *Cryst. Growth Des*. **2012**, 12, 1520−1530. https://doi.org/10.1021/cg201581z
20. Sarcevica, I.; Kons, A.; Orola, L. *Cryst. Eng. Comm.* **2016**, *18*, 1625-1635. https://doi.org/10.1039/C5CE01774B
21. Lemmerer, A.; Bernstein, J.; Kahlenberg, V. *Cryst. Eng. Comm*. **2010**, *12*, 2856–2864. https://doi.org/10.1039/c000473a
22. Lemmerer, A.; Bernstein, J.; Kahlenberg, V. *J. Chem. Cryst. Allogr.* **2011,** *41*, 991–997. https://doi.org/10.1007/s10870-011-0031-9
23. Mashhadi, S. M. A.; Yunus, U.; Bhatti, M. H.; Tahir, M.N. *J. Mol. Struct.* **2014**, *1076*, 446-452. https://doi.org/10.1016/j.molstruc.2014.07.070
24. Oruganti, M.; Khade, P.; Das, U. K.; Trivedi, D.R. *RSC. Adv.* **2016**, *6*, 15868–15876. https://doi.org/10.1039/C5RA14951G
25. Cherukuvada, S.; Nangia, A. *Cryst. Eng. Comm.* **2012**, 14, 2579. https://doi.org/10.1039/c2ce06391c
26. Desiraju, G. R. *Journal of the American Chemical Society* **2013,** *135*, 9952–9967. https://doi.org/10.1021/ja403264c
27. Aakeröy, C. B.; Sinha, A. S. Monographs in Supramolecular Chemistry No. 24 Co-crystals: Preparation, Characterization and Applications, Edited by Christer B. Aakeröy and Abhijeet S. Sinha The Royal Society of Chemistry **2018**, 33 – 79. https://doi.org/10.1039/9781788012874
28. Bhattacharya, S.; Peraka, K. S.; Zaworotko, M. J. Monographs in Supramolecular Chemistry No. 24 Co-crystals: Preparation, Characterization and Applications, Edited by Christer B. Aakero¨y and Abhijeet S. Sinha The Royal Society of Chemistry **2018**, 33 – 79.